

Article

Comparative Analysis of Thin and Thick MoTe₂ Photodetectors: Implications for Next-Generation Optoelectronics

Saddam Hussain , Shaoguang Zhao, Qiman Zhang and Li Tao * 

Center for Quantum Physics, Key Laboratory of Advanced Optoelectronic Quantum Architecture and Measurement (MOE), School of Physics, and Center for Interdisciplinary Science of Optical Quantum and NEMS Integration, Beijing Institute of Technology, Beijing 100081, China; 3820202051@bit.edu.cn (S.H.); zhaoshaoguang@bit.edu.cn (S.Z.); zqm@bit.edu.cn (Q.Z.)

* Correspondence: litao@bit.edu.cn

Abstract: Due to its outstanding optical and electronic properties, molybdenum ditelluride (MoTe₂) has become a highly regarded material for next-generation optoelectronics. This study presents a comprehensive, comparative analysis of thin (8 nm) and thick (30 nm) MoTe₂-based photodetectors to elucidate the impact of thickness on device performance. A few layers of MoTe₂ were exfoliated on a silicon dioxide (SiO₂) dielectric substrate, and electrical contacts were constructed via EBL and thermal evaporation. The thin MoTe₂-based device presented a maximum photoresponsivity of 1.2 A/W and detectivity of 4.32×10^8 Jones, compared to 1.0 A/W and 3.6×10^8 Jones for the thick MoTe₂ device at 520 nm. Moreover, at 1064 nm, the thick MoTe₂ device outperformed the thin device with a responsivity of 8.8 A/W and specific detectivity of 3.19×10^9 Jones. Both devices demonstrated n-type behavior, with linear output curves representing decent ohmic contact amongst the MoTe₂ and Au/Cr electrodes. The enhanced performance of the thin MoTe₂ device at 520 nm is attributed to improved carrier dynamics resulting from effective electric field penetration. In comparison, the superior performance of the thick device at 1064 nm is due to sufficient absorption in the near-infrared range. These findings highlight the importance of thickness control in designing high-performance MoTe₂-based photodetectors and position MoTe₂ as a highly suitable material for next-generation optoelectronics.



Citation: Hussain, S.; Zhao, S.; Zhang, Q.; Tao, L. Comparative Analysis of Thin and Thick MoTe₂ Photodetectors: Implications for Next-Generation Optoelectronics. *Nanomaterials* **2024**, *14*, 1804. <https://doi.org/10.3390/nano14221804>

Academic Editor: Ion Mihailescu

Received: 11 October 2024

Revised: 7 November 2024

Accepted: 8 November 2024

Published: 11 November 2024



Copyright: © 2024 by the authors. Licensee MDPI, Basel, Switzerland. This article is an open access article distributed under the terms and conditions of the Creative Commons Attribution (CC BY) license (<https://creativecommons.org/licenses/by/4.0/>).

Keywords: MoTe₂; photodetectors; optoelectronic performance; thin films; thick films; responsivity

1. Introduction

The growth of innovative photodetectors remains critical for diverse applications, including imaging, optical communication, environmental monitoring, and biomedical sensing [1]. Two-dimensional materials, particularly transition metal dichalcogenides (TMDs), have become capable contenders for next-generation photodetection technologies due to their outstanding optical, electrical, and mechanical characteristics [2]. Among these materials, molybdenum ditelluride (MoTe₂) has expanded significantly due to its adjustable band gap, excellent electron mobility, and excellent photoresponsivity, making it ideal for electronic and optoelectronic devices [3]. MoTe₂ is classified into three distinct structural phases: the semiconducting trigonal-prismatic 2H- or α -phase, the semi-metallic and monoclinic 1T'- or β -phase, and the semi-metallic orthorhombic γ -structure, which allows for diverse expedient configurations and functionalities. The phase tunability and variable thickness-dependent possessions deliver prospects for improving device performance across a broad spectrum of applications [4]. The thickness of MoTe₂ layers significantly affects their optoelectronic characteristics, with thickness-dependent layers often exhibiting superior photoresponse, faster switching times, and enhanced charge carrier dynamics. The survey of contemporary research has merged several schemes to enhance the efficiency of MoTe₂-based photodetectors. In the end, the authors proved that the enhancement of the

photocurrent response sensitivity or detectivity of MoTe₂ photodetectors was achieved by incorporating all-dielectric TiO₂ metalenses. These metalenses enhanced the use of photons in the operation of the device to improve results [5]. However, their attention mainly focused on exploring other external optical architectures to improve the performance, but they did not investigate how the thickness changes the photoresponse of MoTe₂. In another work, a MoTe₂ waveguide photodetector with a few layers was still under consideration; it offered reliable performance in near-infrared (NIR) regions, mainly for high-speed optical data communication [6]. Although this research focused on exceeding the external quantum efficiency of MoTe₂ for NIR applications, it failed to determine the effect of varying material thickness on its efficiency in both the visible and NIR regions. The contribution of our work is made in the comprehensive comparative study of thin (8 nm) and thick (30 nm) MoTe₂ layers regarding the dependence of the device performance on the layer thickness in the visible (520 nm) and near-infrared (1064 nm) regions. In contrast to previous studies, which mainly looked at external modifications or specific wavelength use of MoTe₂, this study systematically investigates the thickness-dependent characteristics of the material. We also show that a few thinner MoTe₂ layers have better device performance at the visible range because of the improved electric field penetration. Conversely, the absorption of light in the thicker layers is superior in the NIR range. It gives significant information about the relationship between the thickness of MoTe₂ and how it can be tuned for different photodetection applications, making it possible to have a different perspective on tuning the MoTe₂ photodetectors. The work presented herein is also novel due to the absence of comparative analysis research focusing on the thickness of the MoTe₂ photodetector. It surpasses prior research by offering specific recommendations for thickness optimization in future device designs. Recent studies have shown that thin MoTe₂ photodetectors demonstrate improved performance metrics, such as higher responsivity, specific detectivity, and faster response times, than thicker layers. These performance improvements are primarily attributed to the higher surface-to-volume ratio, better electric field penetration, and enhanced charge transport properties in thinner layers, facilitating more efficient photogenerated carrier extraction. As a result, optimizing the thickness of MoTe₂ layers becomes a critical parameter in the design and development of high-performance photodetectors [7].

Despite these promising characteristics, systematic studies are still needed on the comparability performance of MoTe₂ photodetectors with varying thicknesses under different operating conditions. Understanding the impact of thickness on critical parameters, for instance, responsivity, detectivity, and response time, is essential for designing and optimizing high-performance devices. Our study comprehensively analyzes thin (8 nm) and thick (30 nm) MoTe₂-based photodetectors fabricated with Au and Cr electrodes on a silicon substrate. We systematically explore the optoelectronic properties of these devices, focusing on their electrical and photoresponse characteristics under dark and illuminated conditions.

Our findings disclose that thin MoTe₂-based photodetectors show superior performance in areas such as responsivity, specific detectivity, and external quantum efficiency, which were 1.2 A/W, 4.32×10^8 Jones, and 285%, respectively, compared to thicker MoTe₂ layers, which were 1.0 A/W, 3.6×10^8 Jones, and 238% at 520 nm, respectively. Similarly, thin photodetectors demonstrated responsivity of 1.1 A/W, specific detectivity of 3.96×10^8 Jones, and EQE of 127%, compared to thick-based MoTe₂, which had photo responsivity of 8.8 A/W, detectivity of 3.19×10^9 Jones, and EQE value of 1027% at 1064 nm. Specifically, the enhanced performance of thin MoTe₂ layers is due to improved carrier dynamics, which result from the effective penetration of the electric field into the material, leading to better charge separation and reduced recombination rates at 520 nm. The improved performance of thick-based MoTe₂ at 1064 nm is because MoTe₂ has sufficient absorption in the (NIR) range because of its reduced energy gap. This study emphasizes the position of exact thickness switches in fabricating MoTe₂-based photodetectors. This performance gap emphasizes the critical impact of material thickness on device efficiency, making it a crucial feature in the engineering of photodetectors for optoelectronic applications. By

strategically manipulating the thickness of MoTe₂, it is possible to tailor its photoresponse properties toward exact application ratios, paving the way for developing next-generation photodetection technologies. This work highlights the potential of thin and thick MoTe₂ photodetectors for high-performance photodetectors and provides valuable insights into the design principles that govern the performance of 2D material-based devices. Our comparative study of thin and thick MoTe₂ photodetectors establishes a foundation for future research to optimize TMD-based devices by strategically manipulating material thickness and heterostructure design.

2. Materials and Methods

The fabrication process for thick- and thin-based MoTe₂ devices begins with the exfoliation of MoTe₂ from a 2H phase provided by Nanjing MKNANO Tech. Co., Ltd., Nanjing, China (www.mukenano.com) (accessed on 15 September 2024). These exfoliated films are, at that moment, carefully positioned on Si, covered by a 285 nm thick SiO₂ film as the dielectric foundation. AFM is employed to conduct a thorough structural examination, determining the precise thickness and configuration of the MoTe₂ sheets. Following this, electrode patterns are created using electron beam lithography (EBL). The final step involves thermal evaporation to deposit a 5 nm chromium (Cr) base layer and a 50 nm gold (Au) upper layer, forming thick and thin MoTe₂-based devices. The thickness and morphology of various MoTe₂ layers were examined using atomic force microscopy (Bruker Multi-Mode 8, Bruker Corporation, Karlsruhe, Germany). Raman spectroscopy analysis (WITec alpha 300R, Oxford Instruments plc, Wiesbaden, Germany) is taken to confirm the thick and thin MoTe₂ structure at an excitation wavelength of 532 nm. A probe stage with a Keithley 2636b semiconductor device analyzer was used to perform electrical measurements on the devices.

3. Results and Discussion

3.1. Structural Features of Thin and Thick MoTe₂

The fabrication process of thin and thick MoTe₂ heterostructure layers commenced with the exact creation of several layers of 2H-phase MoTe₂ onto Si substrate, featuring 285 nm dielectric made from SiO₂, serving as the dielectric layer. The device's electrodes were fabricated using EBL, tracked by the thermal evaporation of Cr and Au films with 5 nm and 50 nm thicknesses, respectively. Figure 1a illustrates the schematic of the MoTe₂ device with two electrodes made of Au and Cr on a SiO₂/Si substrate.

Figure 1b,c shows a photographic and inset AFM image of a thick and thin MoTe₂ photodetector device with Au and Cr electrodes. As indicated in Figure 1d, the thickness of the MoTe₂ nanosheet channel is approximately 8 nm and 30 nm. This suggests that the thin MoTe₂ comprises a few layers, while the thick MoTe₂ is bulky. The thickness root mean square (RMS) values of thick and thin MoTe₂ devices are 6.34 and 2.32 nm, respectively, which confirm that thick surface morphology has greater roughness or variability in its properties compared to thin-based MoTe₂, whose surface is flat, as shown in the inset of Figure 1b,c.

Figure 1e shows the Raman of thick and thin MoTe₂, respectively. Raman shows the changes in responses of both thick and thin MoTe₂ devices for excitation at 532 nm. It shows that three distinctive peaks are observed: the in-plane E_{12g}¹ mode (~232 cm⁻¹), the out-of-plane A_{1g} mode (~171 cm⁻¹), and the bulk in-active B_{12g}¹ phonon mode (~288 cm⁻¹). This latter peak is absent in monolayers, which easily enables their identification for a few layers, as shown in the figure. It confirmed a few layers for thin MoTe₂. Furthermore, in the case of thick MoTe₂, the positions of A_{1g}, E_{12g}¹, and B_{12g}¹ are shifted, with the intensity of E_{12g}¹ and B_{12g}¹ decreasing, and A_{1g} shows a weak signal, which confirms that MoTe₂ is in bulk nature. The sharp, intense peak for the thin layer and the broader, more subdued features for the thick layer align well with known behaviors of MoTe₂ as influenced by its thickness. The result is confirmed in the literature [8].

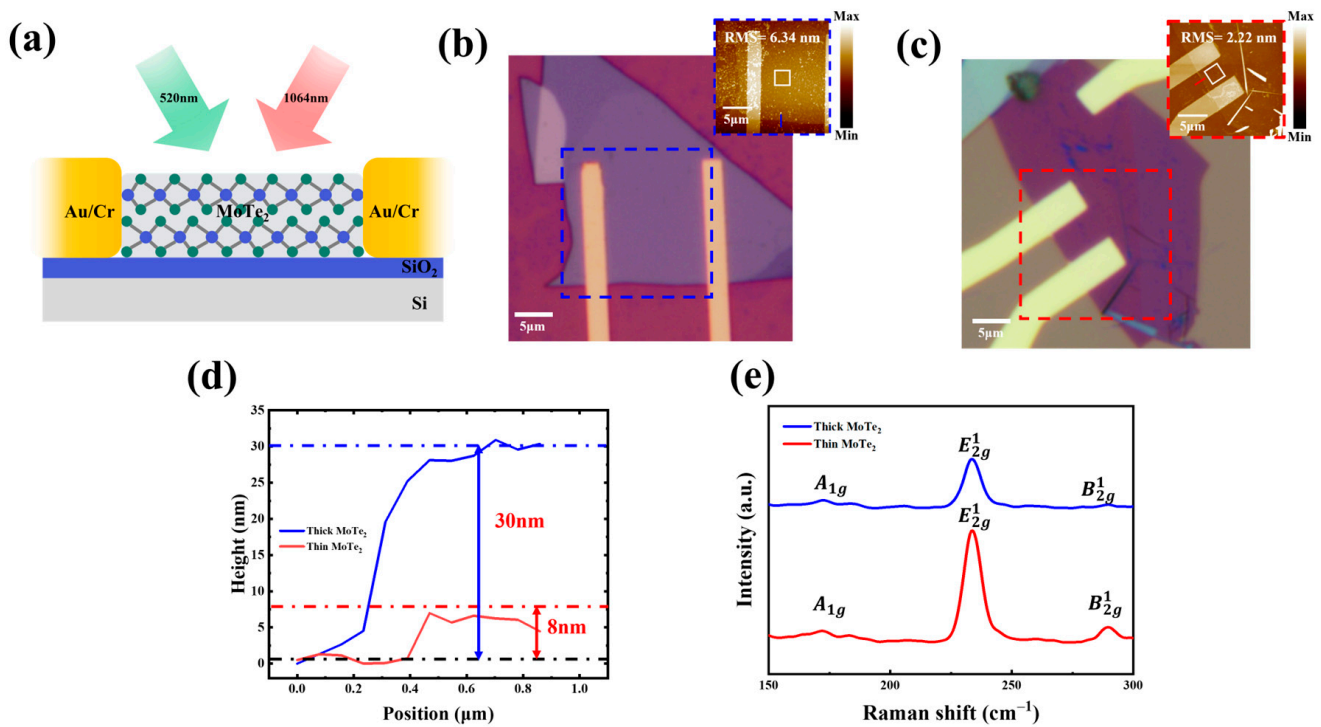


Figure 1. (a) Schematic of the MoTe₂-based photodetector apparatus exposed to light at 520 and 1064 nm. The device comprises MoTe₂ layers on top of a SiO₂/Si substrate coupled with Au/Cr electrodes. (b) Microscopic view of a thick MoTe₂ photodetector through Au/Cr electrodes. (c) Microscopic view of thin MoTe₂ device through Au and Cr electrodes. (d) AFM thickness profile depicting thick and thin MoTe₂ flakes, corresponding to inset in (b,c), with RMS of 6.34 nm and 2.32 nm, respectively. (e) Raman spectra of thick and thin MoTe₂ flakes on SiO₂/Si substrate for the excitation wavelengths of 532 nm.

3.2. Electrical Properties

The output and transfer characteristics were also obtained under different illumination powers, as shown in Figure 2a–d. It indicates a rise in photocurrent with increasing illumination power. The surge in photocurrent with increasing light intensity suggests that the photodetector demonstrates a significant photoconductive effect, which is common in semiconductor materials. The linearity of I_d - V_d characteristic curves shows an outstanding ohmic contact among the MoTe₂ to the Cr electrodes [9]. When exposed to light, the increased current under illumination is due to the production of electron-hole pairs in the MoTe₂ thin film. As the light intensity increases, more charge carriers are created, leading to higher currents. However, the photocurrent variation in a thin-based MoTe₂ photodetector is more significant than that of a thick-based photodetector. This could be due to better light absorption and charge transport properties in the thinner MoTe₂ layer, which can trap and generate more charge carriers than thicker layers. Under dark conditions, the current remains near zero, confirming a low dark current compared to thick-based MoTe₂, as illustrated in Figure 2a–c, which displays the transfer characteristics (I_d versus gate voltage V_g) of the thin MoTe₂ device under dark conditions and illumination (149.64 mW/cm²). Under illumination, the photocurrent increases significantly across the entire range of gate voltages compared to the dark condition, which shows n-type semiconductors. This increase in photocurrent with light results from the photoexcitation of electrons, contributing to the rise in the total current flowing through the device. Similarly, Figure 2c,d shows the transfer characteristics for the thick MoTe₂ device under dark and illuminated conditions, indicating that drain current increases with changing V_g , proving that thick-based MoTe₂ is an n-type semiconductor. As in the thick device, the thin MoTe₂ device shows an increase in photocurrent under light compared to dark conditions. However, there is slight nonlin-

earity in the drain current of thin-based MoTe₂ as light illumination increases, which is because there should be little trap in the thin MoTe₂ layer or interface between MoTe₂ and gate dielectric. However, the overall current values under both dark and light conditions are lower in the thick device compared to the thin one at 520 nm. This suggests lower light absorption and fewer photo-generated carriers in the thick MoTe₂ layer. The thin MoTe₂-based photodetector outperforms the thick MoTe₂ device in terms of photocurrent generation and overall responsiveness to light. The elevated ratio of surface area to volume enhances light absorption and charge transport at 520 nm. It reduces the influence of surface states, making the thin MoTe₂ device more suitable for applications requiring high photocurrent under light exposure.

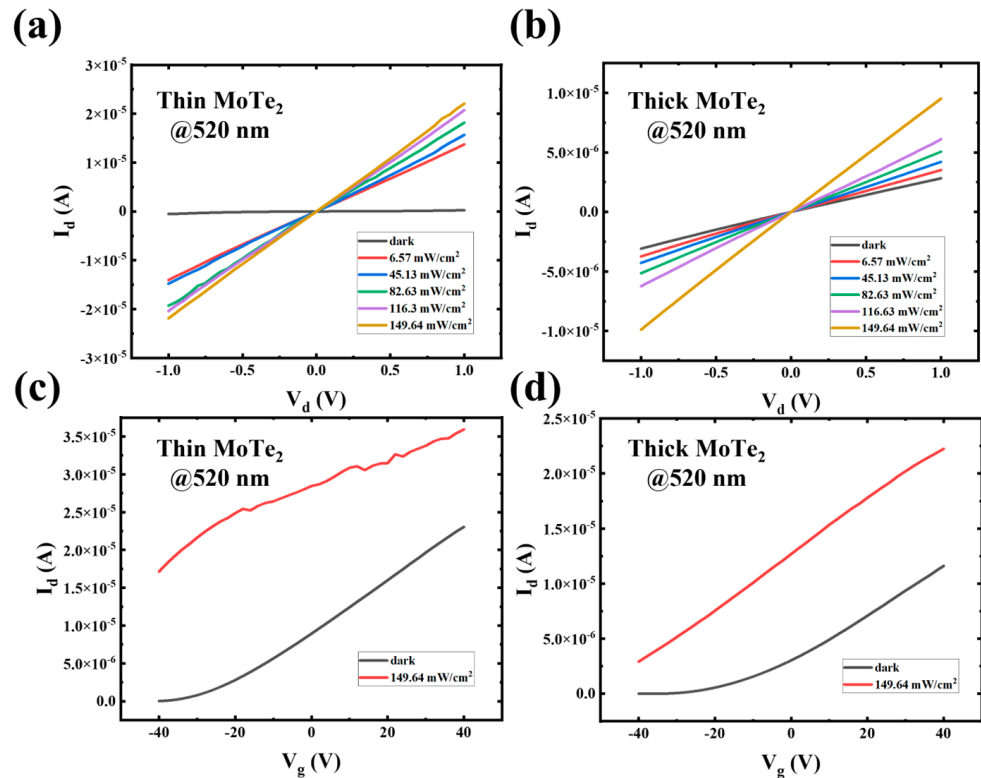


Figure 2. Electrical performance of thin MoTe₂ and thick MoTe₂-based photodetector. (a) Output characteristic curves of thin-based MoTe₂ devices under a wavelength of 520 nm with varying illumination power densities spanning from 6.57 mW/cm² to 149.64 mW/cm². (b) Output characteristic curves of thick-based MoTe₂ device under a wavelength of 520 nm with varying illumination power densities spanning from 6.57 mW/cm² to 149.64 mW/cm². (c) Transfer characteristic curves of thin-based MoTe₂ device under dark and light power density of 149.64 mW/cm² ($V_d = +1$ V). (d) Transfer characteristic curves of thick-based MoTe₂ device under dark and light power density of 149.64 mW/cm² ($V_d = +1$ V).

Figure 3a,b presents the time-dependent photoresponse of the devices operating at V_d of +1 V with periodic light on/off switching. The devices demonstrate a stable and repeatable photocurrent response across the 520 to 1064 nm wavelength range. The photoresponse of thin-based MoTe₂ is improved compared to thick-based MoTe₂ devices at 520 nm, as shown in Figure 3a. This is because MoTe₂ is thinned down to a few atomic layers (monolayer or few layers). It undergoes transitions from having an indirect to direct band gap, significantly enhancing the probability of light absorption and charge carrier generation at visible wavelengths like 520 nm. The tilt observed in the curves in Figure 3a, with differing directions when the light is switched on and off, can be attributed to trap states and interface effects within the MoTe₂ material. The decrease in photocurrent when the light is turned on, followed by a slight increase when the light is off, is due to trap states

and interface effects within the MoTe₂ material. When exposed to light, photogenerated carriers quickly accumulate at defect sites, causing an immediate peak. Over time, these carriers recombine or become further captured at trap states, resulting in a slight decrease in photocurrent even though illumination continues. Similarly, upon switching the light off, the trapped carriers are gradually released, leading to a delayed return to baseline and a tilt in the opposite direction.

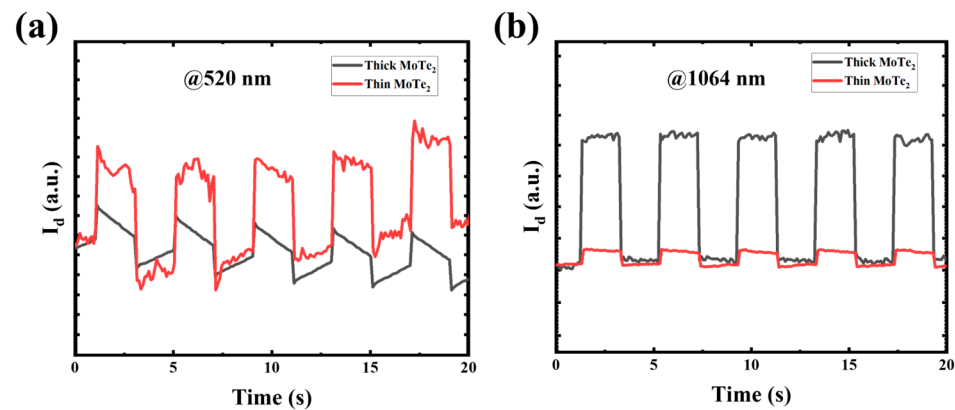


Figure 3. Photoresponses of thick and thin MoTe₂-based devices. (a) Time-dependent photoresponses of thick and thin MoTe₂ at $V_d = +1$ V and $V_g = 0$ V under 520 nm light illumination. (b) Time-dependent photoresponses of thick and thin MoTe₂ at $V_d = +1$ V and $V_g = 0$ V under 1064 nm light illumination.

This behavior reflects the thickness-dependent differences in carrier dynamics between thin and thick MoTe₂ layers, where the varying densities of trap states and surface characteristics influence the speed and direction of response upon light exposure. Conversely, the photoresponse of thick-based MoTe₂ is relatively high compared to thin-based MoTe₂ at 1064 nm, as shown in Figure 3b. This is because thick-based MoTe₂ has sufficient absorption in the NIR range due to its reduced band gap. The higher performance of the thick MoTe₂ device in the NIR range, despite its indirect bandgap, is due to increased optical absorption in thicker layers. The additional thickness allows more effective light trapping, enabling greater absorption of photons in the NIR range, which compensates for the indirect band-to-band transitions that are less efficient.

Our Raman spectroscopy results support this explanation: the broader and shifted Raman peaks in the thick MoTe₂ layer confirm its bulk characteristics and stronger interlayer coupling, which contributes to its indirect bandgap. This structural distinction enhances NIR absorption in thicker layers, allowing for improved photoresponse in this range. Expanding our analysis to measure a broader absorption spectrum for both thick and thin devices would further validate these findings and strengthen the support for the thickness-dependent optical performance of MoTe₂ devices.

The inconsistency in the current versus time response can be attributed to differences in surface defects, trap states, and carrier dynamics between thin and thick MoTe₂ layers. Specifically, thin MoTe₂ layers, with their higher surface-to-volume ratio, tend to have more surface states than trap carriers, resulting in fluctuations in photocurrent. Thicker layers, conversely, exhibit different charge transport properties due to their bulk-like nature, leading to different current behaviors under various light conditions [10]. The rise and decay times are determined by measuring the response times from 10% to 90% and 90% to 10% of the photocurrent when the light source is switched on or off [11]. The rise time constant (τ_{rise}) values are 0.2 and 0.3 s, while the decay time constant (τ_{decay}) values are 0.3 and 0.2 s, respectively, for the MoTe₂ thin and thick-based devices under 520 nm illumination, as demonstrated in Figure 3a. For a comparatively quicker rising time constant of thin-based MoTe₂ and a decay time constant of thick-based MoTe₂ heterostructure device, shown in Figure 3a, in a thin-based MoTe₂ device, the charge carriers exhibit

higher speed compared to those in a thick-based MoTe₂ photodetector. However, this trend is reversed during decay when the thin-based MoTe₂ structure is exposed to light at 520 nm. The slower response times observed in our MoTe₂ devices are primarily due to trap states and surface/interface defects within the material. These imperfections capture photogenerated charge carriers, slowing their recombination and transport, which results in delayed photocurrent decay and slower overall response. Additionally, a MoTe₂-layered structure can contribute to interface effects that impede carrier mobility, further impacting response time. Addressing these limitations through surface passivation techniques, such as an Al₂O₃ or h-BN layer, could potentially reduce trap states and enhance response speed by improving carrier mobility and minimizing recombination delays.

Possible degradation by transfer processes might cause a slow decay time. This is due to the dispersive impact resulting from ionic impurities introduced during the transfer procedure and the deterioration induced by the patterning process. Thick-based MoTe₂ has a significant rise and decay time of 0.1 and 0.2 s, respectively, compared to thin-based MoTe₂, whose rise time and decay time are 0.1 and 0.3 s, respectively, at 1064 nm, as illustrated in Figure 3b. This demonstrates the superior performance of the thick-based MoTe₂ device in photodetection, particularly in high-speed applications at 1064 nm.

This is why optimization of the following factors can significantly improve the photoresponse of MoTe₂ films. First, it has been suggested that the thickness of the MoTe₂ layers could be optimized to yield improved performance for specific wavelengths. Our study shows that thin MoTe₂ layers are better for the 520 nm source, and thicker films work better at 1064 nm because of the dissimilarities of successiveness and band structure. The first possible enhancement is that the absorption efficiency for those wavelengths of interest can be maximized by adjusting layer thickness and increasing responsivity and detectivity. The second possible enhancement relates to surface passivation. Defects and cracks at the surface layer for the thin MoTe₂ films pin the carriers, which in turn results in a decay of photoresponse. A new passivation layer of Al₂O₃ or h-BN could reduce the surface defects, thus improving carrier dynamics and, in return, contributing to the increase in photocurrent [12]. Further, doping or alloying MoTe₂ with elements like Se or S might introduce the means to adjust the bandgap for light absorption and enhance the carrier mobility of the material [13]. This, in turn, would lead to improved photoresponsivity, in particular in certain spectral regions. Another possibility is the enhancement arising from the fusion of MoTe₂ with other 2D materials in heterostructure architectures. The heterostructures also provide a strong possibility of separating the charges as they form built-in potentials at the interfaces to improve the photocurrent and response time. Furthermore, designing sample structures with plasmonic nanostructures like gold/silver nanoparticles introduces a huge local field enhancement due to plasmonic resonance and improves light absorption photo-carrier generation [14]. There is a possibility that the optimization of the metal contacts can significantly enhance the device's performance. The work function difference and contact resistance of the two metal electrodes can be decreased through a selection of metals with closer work functions or insertion of interfacial layers, leading to a decrease in the Schottky barrier and thus improvement in the photoresponse of the device.

Last, an external gate bias may adjust the carrier density in MoTe₂ for better charge separation with enhanced photodetector sensitivity under different lighting conditions. From the investigation of the thickness optimization, surface passivation, doping, heterostructure integration, plasmonic enhancement, contact optimization, and external gating, it can be realized that these methods can enhance the photoresponse of MoTe₂-based photodetectors, and it can thus be more resourceful in sophisticated optoelectronics.

In addition, we carried out essential measurements such as photoresponsivity (R), specific detectivity (D^*), and EQE using the following equations:

$$R = \frac{I_{ph}}{P \times S} \quad (1)$$

$$D^* = R \times \sqrt{\frac{S}{2qI_{dark}}} \quad (2)$$

$$EQE = \frac{hcR}{q\lambda} \times 100\% \quad (3)$$

where I_{ph} represents photocurrent, while I_{dark} denotes dark current. P signifies the incident illumination power density, and S represents the illumination area on the channel. The electron charge is denoted by q , h stands for Planck's constant, c represents the speed of light, and λ indicates the wavelength of incident light [15,16]. At 520 nm, the power density remained 149.64 mW/cm², while at 1064 nm, it was 47 mW/cm², both at a 1 V bias voltage. The thin-based MoTe₂ exhibited enhanced performance through a wavelength of 520 and thick-based MoTe₂ at 1064 nm. At 520 nm, it confirmed a responsivity of 1.2 A/W, a detectivity of 4.32×10^8 Jones, and an EQE of 285%. In contrast, thick-based MoTe₂ showed a photoresponsivity of 1.0 A/W, a detectivity of 3.6×10^8 Jones, and an external quantum efficiency of 238% at the same wavelength. At 1064 nm, the thin MoTe₂ displayed a photoresponsivity of 1.1 A/W, specific detectivity of 3.96×10^8 Jones, and an EQE of 127%. For thick MoTe₂ at this wavelength, the responsivity was 8.8 A/W, specific detectivity was 3.19×10^9 Jones, and EQE was 1027%, indicating superior performance compared to thin-based MoTe₂ at 1064 nm.

We also compared the parameters of our novel thin and thick MoTe₂ photodetectors with those of traditional photodetection devices, as summarized in Table 1.

Table 1. Comparison of photodetectors based on thin and thick MoTe₂ and two-dimensional material-based heterostructures.

Device	Wavelength (nm)	Responsivity (A/W)	Detectivity (Jones)	E.Q.E	Ref.
AgNPs-MoS ₂	980	8.8×10^{-4}	1.28×10^9	-	[17]
WSe ₂	780	7.25×10^{-5}	2.4×10^7	11.55%	[18]
ZnS-MoS ₂	554	1.78×10^{-5}	-	0.4%	[19]
MoS ₂ /PbS	400–1500	4.3×10^2	-	-	[20]
SnS	400–700	4.3×10^{-3}	71×10^6	-	[21]
MoSe ₂	532	1.7×10^{-4}	11.58×10^8	0.025%	[16]
SnS _{0.25} Se _{0.75}	400–700	1.17×10^{-4}	-	-	[22]
MoS ₂ -MoO ₃	405	1.3×10^{-4}	-	0.041%	[23]
GeP	440	1×10^{-5}	1.38×10^7	-	[24]
WS ₂	458	2.12×10^{-6}	-	-	[25]
PbI ₂	450	1.0×10^{-4}	-	-	[26]
PbI ₂	405	1.3×10^{-3}	-	-	[27]
ITO/PbI ₂ /Au	-	0.5×10^{-3}	2.5×10^{12}	-	[28]
MoS ₂	488	4.2×10^{-4}	-	-	[29]
CdTe	473	1.6×10^{-4}	5.84×10^9	-	[30]
MoS ₂	514.5	1.1×10^{-3}	-	-	[31]
MoTe ₂ (thin)	520	1.2	4.32×10^8	285%	This Work
MoTe ₂ (thick)	520	1.0	3.6×10^8	238%	This Work
MoTe ₂ (thin)	1064	1.1	3.96×10^8	127%	This Work
MoTe ₂ (thick)	1064	8.8	3.19×10^9	1027%	This Work

Moreover, Figure 4 displays the charge transfer mechanism of MoTe₂-based devices. The MoTe₂ has diverse Fermi levels with Cr electrodes since Cr electrodes are not in contact with the MoTe₂ channel, as shown in Figure 4a. The valence band maximum of MoTe₂ and the work function of Cr have also been determined to be 4.8 eV [32] and 4.5 eV [33], respectively. In the zero-bias condition (Figure 4b), the Fermi level of MoTe₂ and Cr electrodes is aligned. It remains in equilibrium between the Cr electrodes and the MoTe₂, with no significant band bending, meaning no photocurrent is generated. Upon exposure to light, by applying V_d of -1 V, the MoTe₂ channel absorbs photons, and the electron moves,

leaving the holes in the valence band. Fermi level (E_F) shifts towards the valence band of MoTe₂, creating a substantial energy barrier between the conduction band of MoTe₂ and the Fermi levels of the Cr electrodes. As a result, the electron pairs generate energy that exceeds the bandgap of the MoTe₂ flake, producing additional free charge carriers and diminishing the semiconductor's electrical resistance, as shown in Figure 4c. When applying a +1 V bias voltage, the Fermi level approaches MoTe₂'s conduction band, forming a minor barrier between MoTe₂'s conduction band and the Cr electrodes' Fermi level, as shown in Figure 4d. The application of bias voltage reduces the Schottky barrier height across the junction. The separation of electron-hole pairs results in their rapid movement, where electrons move in opposing directions, and they are gathered by electrodes with Ohmic contact. This process leads to a substantial current (photocurrent) rise between the metal electrodes, effectively traveling to the external circuit and producing a high photocurrent [29,34]. The separation of electron-hole pairs plays a vital role in generating a photocurrent [35,36]. These mechanisms of charge transfer and photo-detection are present across all contacts.

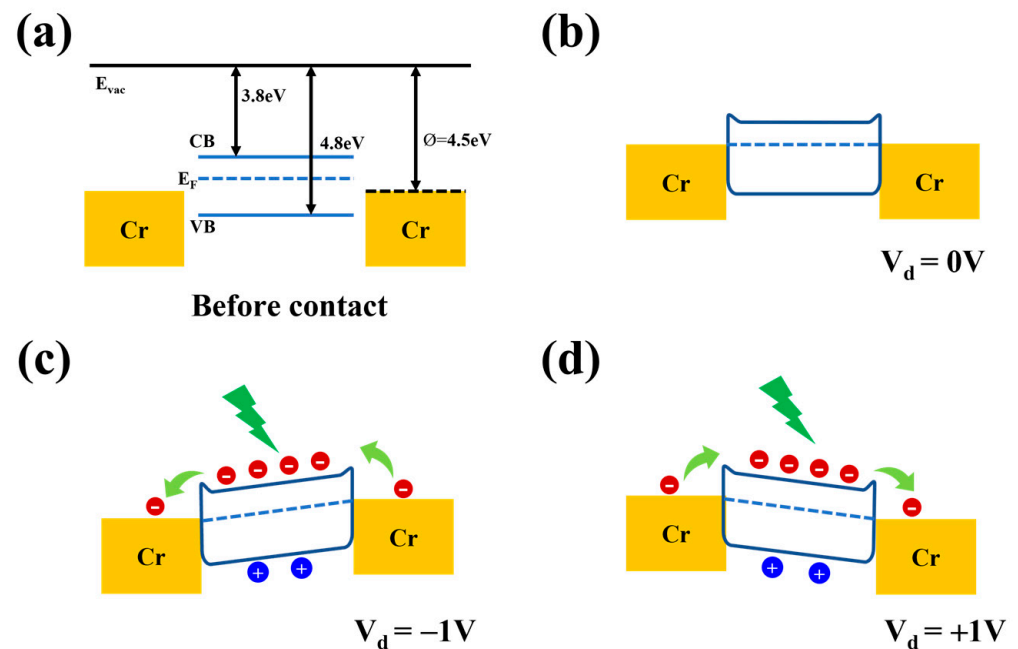


Figure 4. (a) Energy band diagrams of MoTe₂-based photodetectors (E_{vac} represents the vacuum energy, and E_F denotes the Fermi level), with CB indicating the conduction band, VB the valence band, and Φ representing the work function. (b) Carrier transfer at $V_d = 0$. (c) Carrier transfer at applied bias $V_d = -1$ V. (d) Carrier transfer at $V_d = +1$ V.

4. Conclusions

This study discovered the optoelectronic features of MoTe₂-based photodetectors by variable thicknesses, precisely relating thin (8 nm) and thick (30 nm) layers. The thin MoTe₂-based photodetector demonstrated superior responsivity, detectivity, and response time performance compared to thick-based MoTe₂ at 520 nm. This enhanced performance is attributed to the higher surface-to-volume ratio, better electric field penetration, and improved charge transport properties in the thin layers, facilitating more efficient photo-generated carrier extraction. Conversely, thick-based MoTe₂ performs better in responsivity, specific detectivity, and EQE at 1064 nm, as described. The enhanced performance is due to the reduced band gap of thick-based MoTe₂ due to their bulk nature. Both thin and thick MoTe₂-based devices exhibited n-type behavior. Output characteristic curves specified a photoconductive effect through the thick MoTe₂ device, showing a more significant increase in drain current under light illumination, highlighting its better responsiveness to fluctuating light power densities. The study concludes that thickness control is crucial in de-

signing MoTe₂-based photodetectors, with thinner layers at visible and thicker at infrared, providing better sensitivity, faster response times, and improved overall performance. This shows that thickness-dependent MoTe₂ layers are promising candidates for next-generation photodetection technologies, with applications in imaging, optical communications, and other optoelectronic devices. Future research could explore further optimization through material integration and device structure improvements. In summary, our comparative analysis of thin and thick MoTe₂-based photodetectors demonstrates the critical impact of thickness on optoelectronic performance. Thin MoTe₂ layers exhibit superior responsivity in the visible range, while thicker layers excel in the near-infrared region. These findings position MoTe₂ films as promising candidates for next-generation optoelectronic applications, including visible light photodetectors, infrared detectors, flexible electronics, and high-speed optoelectronic devices. Future work will explore the integration of MoTe₂ with other 2D materials and device optimizations for specific applications.

Author Contributions: Conceptualization, S.H. and L.T.; methodology, S.H. and S.Z.; validation, S.Z., Q.Z. and L.T.; formal analysis, S.H., S.Z. and L.T.; investigation, S.H. and S.Z.; resources, L.T.; data curation, S.Z. and Q.Z.; writing—original draft preparation, S.H.; writing—review and editing, L.T., S.Z. and Q.Z.; visualization, S.Z.; supervision, L.T.; project administration, L.T.; funding acquisition, L.T. All authors have read and agreed to the published version of the manuscript.

Funding: This work was sponsored by the National Key Research and Development Program of China under Grant No. 2023YFB3208002, the National Natural Science Foundation of China under Grant No. 62005051, the Key Laboratory of Photoelectric Imaging Technology and System (Ministry of Education), the Analysis & Testing Center at the Beijing Institute of Technology, and the start-up fund provided by the Beijing Institute of Technology.

Data Availability Statement: Specific features of the study and the original findings are described in the article; if you have any other questions, they should be addressed to the corresponding author.

Conflicts of Interest: The authors have disclosed no potential conflicts of interest.

References

1. Konstantatos, G. Current Status and Technological Prospect of Photodetectors Based on Two-Dimensional Materials. *Nat. Commun.* **2018**, *9*, 5266. [[CrossRef](#)] [[PubMed](#)]
2. Huo, N.; Konstantatos, G. Recent Progress and Future Prospects of 2D-Based Photodetectors. *Adv. Mater.* **2018**, *30*, 1801164. [[CrossRef](#)] [[PubMed](#)]
3. Shinde, P.V.; Hussain, M.; Moretti, E.; Vomiero, A. Advances in Two-Dimensional Molybdenum Ditelluride (MoTe₂): A Comprehensive Review of Properties, Preparation Methods, and Applications. *SusMat* **2024**, *4*, e236. [[CrossRef](#)]
4. Rhodes, D.; Chenet, D.A.; Janicek, B.E.; Nyby, C.; Lin, Y.; Jin, W.; Hone, J.; Balicas, L. Engineering the Structural and Electronic Phases of MoTe₂ Through W Substitution. *Nano Lett.* **2017**, *17*, 1616–1622. [[CrossRef](#)]
5. Qiao, J.; Feng, F.; Cao, G.; Wei, S.; Song, S.; Wang, T.; Somekh, M.G. Ultrasensitive Near-Infrared MoTe₂ Photodetectors with Monolithically Integrated Fresnel Zone Plate Metalens. *Adv. Opt. Mater.* **2022**, *10*, 2200375. [[CrossRef](#)]
6. Ma, P.; Flory, N.; Salamin, Y.; Bäuerle, B.; Emboras, A.; Josten, A.; Leuthold, J. Fast MoTe₂ Waveguide Photodetector with High Sensitivity at Telecommunication Wavelengths. *ACS Photonics* **2018**, *5*, 1846–1852. [[CrossRef](#)]
7. Cong, X.; Shah, M.N.U.; Zheng, Y.; He, W. Largely Reducing the Contact Resistance of Molybdenum Ditelluride by In Situ Potassium Modification. *Adv. Electron. Mater.* **2023**, *9*, 2300062. [[CrossRef](#)]
8. Yamamoto, M.; Wang, S.T.; Ni, M.; Lin, Y.F.; Li, S.L.; Aikawa, S.; Jian, W.B.; Ueno, K.; Wakabayashi, K.; Tsukagoshi, K. Strong enhancement of Raman scattering from a bulk-inactive vibrational mode in few-layer MoTe₂. *ACS Nano* **2014**, *8*, 3895–3903. [[CrossRef](#)]
9. Cheng, Y.; Qiu, Z.; Zhao, S.; Zhang, Q.; Zhao, J.; Zi, X.; Zhao, Y.; Zheng, Z.; Tao, L. Multifunctional Optoelectronic Devices Based on Two-Dimensional Tellurium/MoS₂ Heterojunction. *Appl. Phys. Lett.* **2024**, *125*, 171105. [[CrossRef](#)]
10. Ji, H.; Joo, M.K.; Yun, Y.; Park, J.H.; Lee, G.; Moon, B.H.; Lim, S.C. Suppression of Interfacial Current Fluctuation in MoTe₂ Transistors with Different Dielectrics. *ACS Appl. Mater. Interfaces* **2016**, *8*, 19092–19099. [[CrossRef](#)]
11. Basumatary, P.; Agarwal, P. Photocurrent Transient Measurements in MAPbI₃ Thin Films. *J. Mater. Sci. Mater. Electron.* **2020**, *31*, 10047–10054. [[CrossRef](#)]
12. Sirota, B.; Glavin, N.; Krylyuk, S.; Davydov, A.V.; Voevodin, A.A. Hexagonal MoTe₂ with Amorphous BN Passivation Layer for Improved Oxidation Resistance and Endurance of 2D Field Effect Transistors. *Sci. Rep.* **2018**, *8*, 8668. [[CrossRef](#)] [[PubMed](#)]
13. Yao, J.; Yang, G. 2D Layered Material Alloys: Synthesis and Application in Electronic and Optoelectronic Devices. *Adv. Sci.* **2022**, *9*, 2103036. [[CrossRef](#)]

14. Tao, L.; Chen, Z.F.; Li, Z.Y.; Wang, J.Q.; Xu, X.; Xu, J.-B. Enhancing light-matter interaction in 2D materials by optical micro/nano architectures for high-performance optoelectronic devices. *InfoMat* **2021**, *3*, 36–60. [[CrossRef](#)]
15. Wazir, N.; Liu, R.; Ding, C.; Wang, X.; Ye, X.; Lingling, X.; Lu, T.; Wei, L.; Zou, B. Vertically Stacked MoSe₂/MoO₂ Nanolayered Photodetectors with Tunable Photoresponses. *ACS Appl. Nano Mater.* **2020**, *3*, 7543–7553. [[CrossRef](#)]
16. Wazir, N.; Zhang, M.; Li, L.; Ji, R.; Li, Y.; Wang, Y.; Ma, Y.; Ullah, R.; Aziz, T.; Cheng, B.; et al. Three-Terminal Photodetectors Based on Chemical Vapor Deposition-Grown Triangular MoSe₂ Flakes. *FlatChem* **2022**, *34*, 100399. [[CrossRef](#)]
17. Park, M.J.; Park, K.; Ko, H. Near-Infrared Photodetector Achieved by Chemically-Exfoliated Multilayered MoS₂ Flakes. *Appl. Surf. Sci.* **2018**, *448*, 64–70. [[CrossRef](#)]
18. Patel, R.P.; Pataniya, P.M.; Patel, M.; Sumesh, C.K. WSe₂ Crystals on Paper: Flexible, Large Area, and Broadband Photodetectors. *Nanotechnology* **2021**, *32*, 505202. [[CrossRef](#)]
19. Gomathi, P.T.; Sahatiya, P.; Badhulika, S. Large-Area, Flexible Broadband Photodetector Based on ZnS–MoS₂ Hybrid on Paper Substrate. *Adv. Funct. Mater.* **2017**, *27*, 1701611. [[CrossRef](#)]
20. Kufer, D.; Nikitskiy, I.; Lasanta, T.; Navickaite, G.; Koppens, F.H.L.; Konstantatos, G. Hybrid 2D-0D MoS₂-PbS Quantum Dot Photodetectors. *Adv. Mater.* **2015**, *27*, 176–180. [[CrossRef](#)]
21. Reddy, T.S.; Kumar, M.C.S. Co-Evaporated SnS Thin Films for Visible Light Photodetector Applications. *RSC Adv.* **2016**, *6*, 95680–95692. [[CrossRef](#)]
22. Jethwa, V.P.; Patel, K.; Pathak, V.M.; Solanki, G.K. Enhanced Electrical and Optoelectronic Performance of SnS Crystal by Se Doping. *J. Alloys Compd.* **2021**, *883*, 160941. [[CrossRef](#)]
23. Wei, Y.; Tran, V.T.; Zhao, C.; Liu, H.; Kong, J.; Du, H. Robust Photodetectable Paper from Chemically Exfoliated MoS₂-MoO₃ Multilayers. *ACS Appl. Mater. Interfaces* **2019**, *11*, 21445–21453. [[CrossRef](#)] [[PubMed](#)]
24. Yu, T.; Nie, H.; Wang, S.; Zhang, B.; Zhao, S.; Wang, Z.; Tao, X. Two-Dimensional GeP-Based Broad-Band Optical Switches and Photodetectors. *Adv. Opt. Mater.* **2020**, *8*, 1901490. [[CrossRef](#)]
25. Perea-López, N.; Elias, A.L.; Berkdemir, A.; Castro-Beltran, A.; Gutiérrez, H.R.; Feng, S.; Lv, R.; Hayashi, T.; López-Urías, F.; Ghosh, S.; et al. Photosensor Device Based on Few-Layered WS₂ Films. *Adv. Funct. Mater.* **2013**, *23*, 5511–5517. [[CrossRef](#)]
26. Zheng, W.; Zhang, Z.; Lin, R.; Xu, K.; He, J.; Huang, F. High-Crystalline 2D Layered PbI₂ with Ultrasoft Surface: Liquid-Phase Synthesis and Application of High-Speed Photon Detection. *Adv. Electron. Mater.* **2016**, *2*, 1600291. [[CrossRef](#)]
27. Frisenda, R.; Island, J.O.; Lado, J.L.; Giovanelli, E.; Gant, P.; Nagler, P.; Castellanos-Gomez, A. Characterization of Highly Crystalline Lead Iodide Nanosheets Prepared by Room-Temperature Solution Processing. *Nanotechnology* **2017**, *28*, 455703. [[CrossRef](#)]
28. Saleem, M.I.; Chandrasekar, P.; Batool, A.; Lee, J.H. Aqueous-Phase Formation of Two-Dimensional PbI₂ Nanoplates for High-Performance Self-Powered Photodetectors. *Micromachines* **2023**, *14*, 1949. [[CrossRef](#)]
29. Yin, Z.; Li, H.; Li, H.; Jiang, L.; Shi, Y.; Sun, Y.; Lu, G.; Zhang, Q.; Chen, X.; Zhang, H. Single-Layer MoS₂ Phototransistors. *ACS Nano* **2012**, *6*, 74–80. [[CrossRef](#)]
30. Cheng, R.; Wen, Y.; Yin, L.; Wang, F.; Wang, F.; Liu, K.; He, J. Ultrathin Single-Crystalline CdTe Nanosheets Realized via van der Waals Epitaxy. *Adv. Mater.* **2017**, *29*, 1703122. [[CrossRef](#)]
31. Perea-López, N.; Lin, Z.; Pradhan, N.R.; Iñiguez-Rábago, A.; Elías, A.L.; McCreary, A.; Lou, J.; Ajayan, P.M.; Terrones, H.; Balicas, L.; et al. CVD-Grown Monolayered MoS₂ as an Effective Photosensor Operating at Low-Voltage. *2D Mater.* **2014**, *1*, 011004. [[CrossRef](#)]
32. Shi, W.; Ye, J.; Zhang, Y.; Suzuki, R.; Yoshida, M.; Miyazaki, J.; Iwasa, Y. Superconductivity Series in Transition Metal Dichalcogenides by Ionic Gating. *Sci. Rep.* **2015**, *5*, 12534. [[CrossRef](#)] [[PubMed](#)]
33. Wang, Z.; Wang, F.; Yin, L.; Huang, Y.; Xu, K.; Wang, F.; He, J. Electrostatically Tunable Lateral MoTe₂ p–n Junction for Use in High-Performance Optoelectronics. *Nanoscale* **2016**, *8*, 13245–13250. [[CrossRef](#)] [[PubMed](#)]
34. Hao, Y.; Meng, G.; Ye, C.; Zhang, L. Reversible Blue Light Emission from Self-Assembled Silica Nanocords. *Appl. Phys. Lett.* **2005**, *87*, 031912. [[CrossRef](#)]
35. Lee, J.; Tao, L.; Parrish, K.N.; Hao, Y.; Ruoff, R.S.; Akinwande, D. Multi-Finger Flexible Graphene Field Effect Transistors with High Bendability. *Appl. Phys. Lett.* **2012**, *101*, 252109. [[CrossRef](#)]
36. Lee, H.; Ahn, J.; Im, S.; Kim, J.; Choi, W. High-Responsivity Multilayer MoSe₂ Phototransistors with Fast Response Time. *Sci. Rep.* **2018**, *8*, 11545. [[CrossRef](#)]

Disclaimer/Publisher’s Note: The statements, opinions and data contained in all publications are solely those of the individual author(s) and contributor(s) and not of MDPI and/or the editor(s). MDPI and/or the editor(s) disclaim responsibility for any injury to people or property resulting from any ideas, methods, instructions or products referred to in the content.